



“Electroless” deposition of a pre-film of electrophoresis coating and its corrosion resistance on a Mg alloy

Guang-Ling Song*

Chemical Sciences and Materials Systems Laboratory, GM Research and Development Center, Mail Code: 480-106-212, 30500 Mound Road, Warren, MI 48090, United States

ARTICLE INFO

Article history:

Received 21 September 2009

Received in revised form

22 November 2009

Accepted 23 November 2009

Available online 3 December 2009

Keywords:

Magnesium

Corrosion

Protection

Coating

Surface treatment

ABSTRACT

Magnesium has unique electrochemical performance, which can be utilized in its coating or surface treatment. In this study, a new self-deposited coating process is explored for magnesium alloys. It is found that a thin film can be rapidly formed on a Mg alloy AZ91D through simply dipping the alloy coupon in an E-coating bath solution without applying a current or potential that is essentially required in a normal E-coating process. The “electroless” deposition mechanism and the film growth kinetics are investigated and the formed pre-film of E-coating is evaluated for its stability and corrosion protection performance in a phosphating acidic electrolyte and a NaCl corrosive solution. It is believed that the surface alkalization effect of magnesium is responsible for the “electroless” deposition of the pre-film. The diffusion of hydroxyls in the porous film is controlling the growth of the pre-film. The rapidly formed pre-film can offer sufficient corrosion protection for the magnesium alloy in a chloride-containing environment and it is also stable enough to enable a magnesium alloy part to go through a phosphating bath in a paint line.

© 2009 Elsevier Ltd. All rights reserved.

1. Introduction

Mg and its alloys have many outstanding properties, such as: low density, high strength, great damping capability, excellent casting fluidity, good electric shielding effect, no magnetism, satisfactory heat-conductivity, low heat capacity, acceptable recyclability and no toxicity. In the automotive industry where mass reduction has become a critical issue, the high strength/weight ratio has made Mg alloys a particularly promising alternative to aluminum alloys [1–5].

However, Mg alloys do not have high corrosion resistance and thus many ambitious applications of the existing Mg alloys are currently unrealistic [5]. Various surface treatments and coating techniques have been proposed and developed for magnesium alloys [6,7], such as surface conversion (e.g., chromating and phosphating), anodizing (DOW 17, HAE, Anomag, Keronite, Tagnite, Magoxid); galvanizing/plating (Zn, Cu, Ni, Cr), CVD, PVD, flame or plasma spraying, laser/electron/ion beam treatment, hot-diffusion alloying, and sol–gel coating. Generally speaking, conversion coating and electroless plating are the simplest surface treatments, but they do not offer sufficient corrosion protection for Mg alloys. Other surface treatments and coatings, although more corrosion resistant, are complicated and expensive. Therefore, it would

be of great significance from a practical point of view to have a corrosion resistant coating formed on Mg alloy parts simply through a dipping process like conversion coating or electroless plating.

E-coating (also known as Electrocoating or electrophoresis coating) is a process of using an anodic or cathodic current to apply paint on metallic part surfaces. Cathodic E-coating is a popular process in the automotive industry due to its excellent corrosion resistance and great covering ability on complex metallic components. As E-coat is a great oxygen and moisture barrier [8], it is used as one of the most important layers in coating systems for many applications. However, an E-coating process is relatively complicated in terms of its electrical control and bath solution maintenance. The required current or voltage applied during the deposition step can incur extra operating cost and lead to a “throwing power” (the ability of depositing an E-coat in a recessed area) issue in some deep recessed areas.

To overcome these drawbacks, an innovative “electroless” E-coating technique was recently proposed for Mg alloys [9,10]. The “electroless” E-coating film in nature is a cured E-coating layer that is rapidly (in a few seconds) deposited on a Mg alloy surface from an E-coating bath without applying a current or potential. Therefore, this new coating technique has great advantages over other coatings or surface treatments in terms of the corrosion protection performance, application, operation and maintenance.

The previous publications [9,10] have proposed a simple model to explain the “electroless” deposition process and experimentally

* Tel.: +1 586 986 1339; fax: +1 586 986 9204.

E-mail address: Guangling.song@gm.com.

demonstrated the corrosion protectiveness of the “electroless” E-coat in a NaCl solution. However, as a coating converted from a pre-film of an “electroless” deposited E-coat after curing, the corrosion performance of the “electroless” E-coat is critically determined by its pre-film, which has not been carefully investigated previously. A study on this pre-film can lead to a more comprehensive understanding of the new “electroless” E-coating technique and performance. This paper will present some preliminary results of a study on “electroless” deposition kinetics and corrosion performance of a pre-film.

2. Experimental

2.1. “Electroless” deposition of pre-film of E-coating

Die-cast AZ91D magnesium alloy plates were used in the study. The specimens were manually polished with sand paper up to 1200 grit without using water. Some of the polished bare AZ91D specimens were used as control samples in the following tests. The others were immersed in a cathodic E-coat bath solution containing 16–26 wt% epoxy resin (the main composition of the E-coating bath) and 1.3 wt% titanium dioxide (the pigment that will be deposited together with the resin) at room temperature for a certain period of time. Each of the specimens having been dipped in the E-coating bath solution was then pulled out of the solution slowly so that the solution from its surface gradually flowed back to the bath in order to obtain a stain-free surface. The dipping process resulted in a thin film rapidly formed on the specimen surface. The pre-film covered specimens, after rinsed with de-ionized water, were measured and tested directly.

2.2. *In situ* AC impedance characterization

To better understand the “electroless” deposition mechanism of the pre-film of E-coating, after freshly polished AZ91D coupons were dipped into the E-coating bath, their AC electrochemical impedance spectra (EIS) were immediately and directly measured in the E-coating bath (in a beaker). The specimen served as a working electrode in the bath with a saturated Ag/AgCl electrode as a reference and a Pt foil as a counter electrode. A Solartron electrochemical system, Mode SI1280, was used. EIS measurements of the specimen were repeatedly carried out at their open-circuit potentials at different immersion times in the E-coating bath solution. The amplitude of AC potential signals used in the measurement was 5 mV and the set frequency range was 0.033–17,777 Hz.

As the measurement of a normal AC impedance spectrum takes quite a few minutes to complete, the electrode surface state may change during the measurement or between two successive measurements. To better monitor the impedance during the “electroless” disposition, a quick continuous measurement of impedance $Z_{10\text{Hz}}$ at a fixed frequency ($f=10\text{Hz}$) was also carried out on the specimens in the E-coating bath solution. A 5 mV AC potential signal was used in this test.

2.3. Detection of pre-film

The outer surface of the pre-film of “electroless” E-coating was examined under a microscope. To reveal the interior microstructure, a coated coupon was cut with a diamond saw to obtain its cross-section for SEM examination. The thickness of the pre-films formed after immersion in the E-coating bath for different periods of time was measured using a Multi-measurement System (Fischerscope, an eddy-current coating thickness meter).

2.4. Immersion tests

To evaluate the protectiveness of the pre-film of “electroless” E-coating, specimens coated with a pre-film of “electroless” E-coating that was formed by dipping in the E-coating bath for about ~10 s were immersed in a 5 wt% NaCl solution for 24 h. At the same time, bare AZ91D coupons were also immersed as a control for comparison purpose. Corroded specimens were cleaned with de-ionized water and dried in air. The final corrosion morphologies of the samples were recorded.

It is also important to evaluate the stability of this pre-film of “electroless” E-coating in a phosphating solution. This is because in practical applications a coated Mg alloy part may experience a phosphating surface treatment together with other metal parts. For example, in the automotive industry, the whole vehicle body made of steel, galvanized steel, aluminum and magnesium alloys has to be immersed in a phosphate bath for phosphating treatment before painting. Therefore, in this study, bare AZ91D specimens and the coupons coated with a pre-film that was formed by dipping in the E-coating solution for about ~10 s were immersed in a phosphating bath solution (phosphoric acid 10–30 wt%, zinc oxide 3–7 wt%, nitric acid 1–5 wt%, manganese oxide 1–5 wt%, nickel nitrate 1–5 wt%, potassium fluoride 1–5 wt%, pH 1.5) at room temperature for 4 h. Each of the coupons was covered under a funnel. A burette that was pre-filled with the phosphating bath solution was vertically mounted over the funnel. This set-up allowed the specimen to dissolve under the funnel, and the hydrogen bubbles generated from the coupon surfaces as a result of the dissolution of Mg were led by the funnel into the burette, displacing the solution inside the burette. The decreasing solution level in the burette reflected the amount of hydrogen generated. Detailed description of this set-up was given elsewhere [11]. As the hydrogen evolution rate is proportional to the corrosion rate of the coupon, the overall corrosion amount and rate of the coupon corrosion can be monitored by simply measuring the evolved hydrogen volume [1]. After the immersion in the phosphating solution, specimens were washed with de-ionized water and dried. Their surface morphologies were photographed. Approximately 10 ml of the phosphating solution after the immersion was sampled, which was mixed with 5 ml of hydrochloric acid in a beaker. This solution was then filtered to remove any precipitate and analyzed by ICP-OES (Inductively Coupled Plasma-Optical Emission Spectrometer) for the amount of dissolved Mg ions.

2.5. Electrochemical measurement in 5 wt% NaCl solution

AZ91D coupons coated with pre-films that were formed by dipping the coupons in the E-coating bath for different periods of time were placed in an electrolytic cell containing a 5 wt% NaCl solution for AC impedance and polarization curve (PC) measurements. In this cell, each of the specimens served as a working electrode with a saturated Ag/AgCl electrode as a reference and a Pt foil as a counter electrode. The specimen was exposed to the NaCl solution for 5 min to attain a relatively steady condition before AC impedance measurement. During the AC impedance test, the specimen was held at the open-circuit potential and 5 mV AC potential signals were applied with frequency ranging from 0.033 Hz to 17,777 Hz. After the AC impedance measurement, the specimen was kept in the solution at its open-circuit potential for 2 min for further stabilization, and then potentiodynamic polarization curve measurement was carried out with a potential scanning rate 10 mV/min from cathodic to anodic. The same Solartron electrochemical measurement system for the AC impedance measurement in the E-coating bath was used in the AC impedance and polarization curve measurements. A bare AZ91D coupon was also measured for its AC

impedance and polarization curve under the same testing conditions for comparison.

3. Results

3.1. The pre-film of “electroless” E-coating

After a polished AZ91D specimen was pulled slowly out from the E-coating bath solution, its surface dried quickly in a few seconds. Obviously, the quick drying phenomenon cannot be a physical water evaporation process. It could be a kind of chemical reaction between Mg and the E-coating bath solution on the surface. This quick drying process did not occur on a steel, Al or an Zn specimen under the same conditions after dipping in the same E-coating bath. Their surfaces remained wet for a long time (at least 10 min) after being pulled out from the bath. After washing their surfaces returned to their original states. It should also be noted that the quick drying phenomenon did not occur either if a Mg alloy surface was polished with an aqueous liquid or it had been washed with water after polishing.

After the surface dried, subsequent water rinsing cannot wet the surface any more and water could not stay on the specimen surface at all. This suggests that the surface became highly hydrophobic. The surface morphologies of an AZ91D specimen before and after dipping in the E-coating bath solution are compared in Fig. 1. It is clearly shown that a very thin, uniform and nearly transparent film is formed on the immersed section of the AZ91D surface, which cannot even conceal the original scratches on the substrate.

Fig. 2 reveals the micro-morphology and microstructure of the pre-film of “electroless” E-coating formed on AZ91D being dipped in the E-coating bath solution for ~10 s. Again, the pre-film under the optical microscope is uniform and clearly transparent (Fig. 2(a)), which further confirms the transparency of the film observed by naked eye (Fig. 1). The pre-film is so transparent that the scratches underneath the film on the substrate can be clearly shown (Fig. 2(a)). The topographic view of the pre-film under SEM (Fig. 2(b)) shows that the surface of the film is relatively uniform. However, from the cross-section of the film (Fig. 2(c)), a few tiny pores or defects can be detected in the film. The thickness of the pre-film is about 1.8–2 μm according to the SEM photo (Fig. 2(c)).

The thickness of the pre-films of “electroless” E-coating formed by dipping AZ91D in the E-coating bath solution for various periods

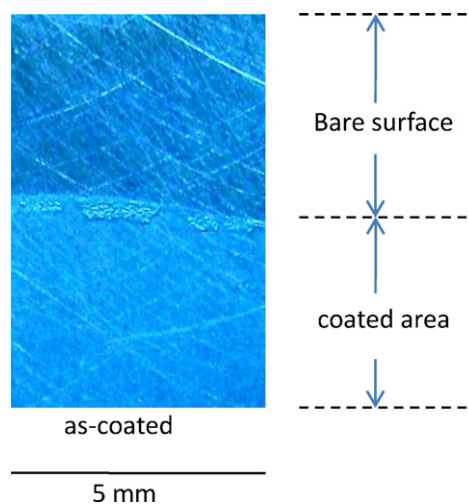


Fig. 1. Comparison of an AZ91D surface with and without a pre-film of “electroless” E-coating (The pre-film was formed by dipping in an E-coating bath solution for 10 seconds).

of time is presented in Fig. 3. It is shown that the pre-film grows with dipping time, and its thickness appears to be a power function of dipping time. When the dipping time is 10 s, the measured thickness of the pre-film is around 1.9 μm , in good agreement with that measured from the SEM cross-section (Fig. 2(c)).

3.2. Impedance characteristics in E-coating bath solution

The “electroless” deposition process of a pre-film of E-coating on AZ91D in the E-coating bath solution was monitored by AC impedance. The measured AC impedance spectra (EISs) of AZ91D after being dipped in the E-coating bath for 1 min, 5 min and 30 min are presented in Fig. 4 (the dot points are experimentally measured data), which shows that there are at least two-capacitive loops in the EISs and the overall impedance increases with dipping time.

A simple equivalent circuit as shown in Fig. 5(a) is used to fit the EIS spectra. For a better fitting result, a constant-phase element Q is used in the equivalent instead of a pure capacitance C . Q can be defined by a capacitance value Q_C and a phase angle index Q_p . The

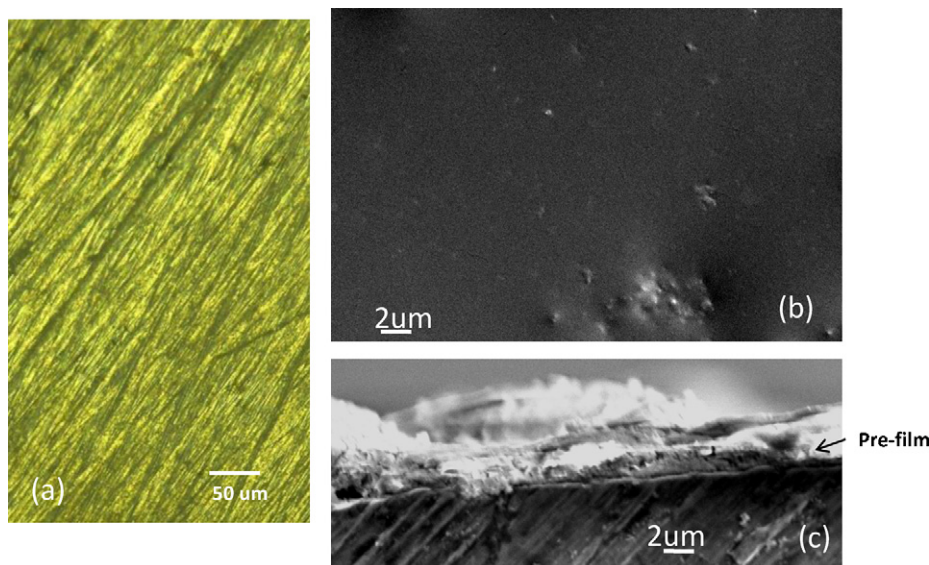


Fig. 2. Surface micro-morphologies of the pre-film of “electroless” E-coating formed on AZ91D by dipping in an E-coating bath solution for 10 s (a) topographic optical observation, (b) topographic SEM observation, (c) cross-section SEM observation.

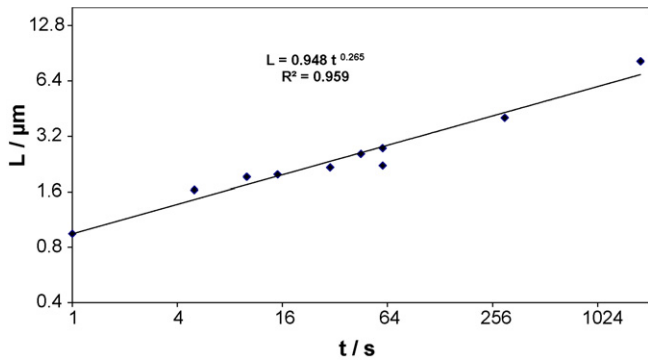


Fig. 3. Dependence of the thickness of a pre-film of “electroless” E-coating on dipping time in an E-coating bath solution.

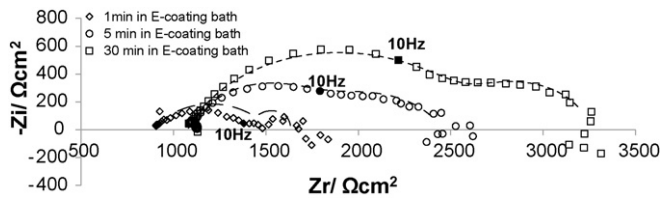


Fig. 4. AC impedance spectra of AZ91D being dipped in an E-coating bath solution for 1 min, 5 min and 30 min, respectively.

fitted EIS spectra (those dash curves) are also plotted in Fig. 4. An explanation of the physic–chemical model of this equivalent circuit will be given after the pre-film formation mechanism and growth kinetics are analyzed in the discussion section. The estimated elements of the equivalent circuit through fitting the measured EISs are listed in Table 1. It is clearly shown that the high frequency impedance R_1 and the total impedance ($R_1 + R_2$) of the system both increase with dipping time.

The increasing high frequency impedance with dipping time can be indirectly verified through monitoring the impedance ($Z_{10\text{Hz}}$) of the pre-film deposition process at a fixed frequency 10 Hz in the E-coating bath (see Fig. 6). The impedance ($Z_{10\text{Hz}}$) measured at this frequency is the impedance as indicated by a solid point in Fig. 4, which is close to ($R_s + R_1$). Fig. 6 shows that the fixed frequency impedance $Z_{10\text{Hz}}$ increasing with dipping time also appears to follow a power function.

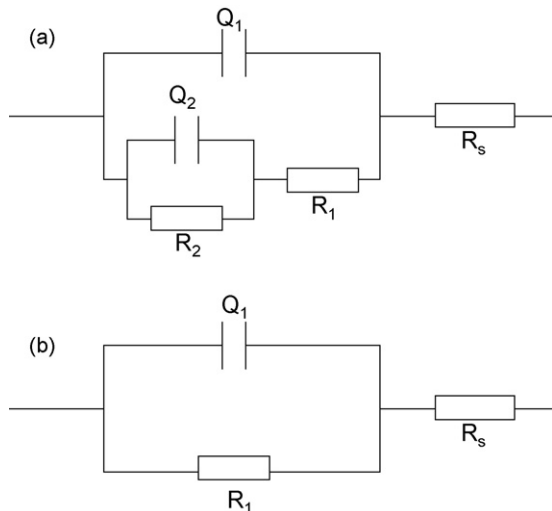


Fig. 5. Equivalent circuits for fitting the EISs in (a) Fig. 4 and (b) Fig. 7.

Table 1

Estimated elements of the equivalent circuit by fitting the EISs (referring to Fig. 4) of AZ91D being dipped in the E-coating bath for various periods of time.

| Circuit elements | Dipping time | | |
|---------------------------------------|--------------|-------|---------|
| | 1 min | 5 min | 30 min |
| R_1 ($\Omega \text{ cm}^2$) | 612 | 767 | 1610 |
| Q_{r1} ($\mu\text{F cm}^{-2}$) | 33 | 11 | 15 |
| Q_{p1} | 0.69 | 0.88 | 0.76 |
| R_2 ($\Omega \text{ cm}^2$) | 128 | 568 | 566 |
| Q_{r2} ($\mu\text{F cm}^{-2}$) | 708 | 336 | 681 |
| Q_{p2} | 1.27 | 0.75 | 0.92 |
| R_s ($\Omega \text{ cm}^2$) | 897 | 1110 | 1080 |
| $R_1 + R_2$ ($\Omega \text{ cm}^2$) | 1510 | 1880 | 2690.76 |

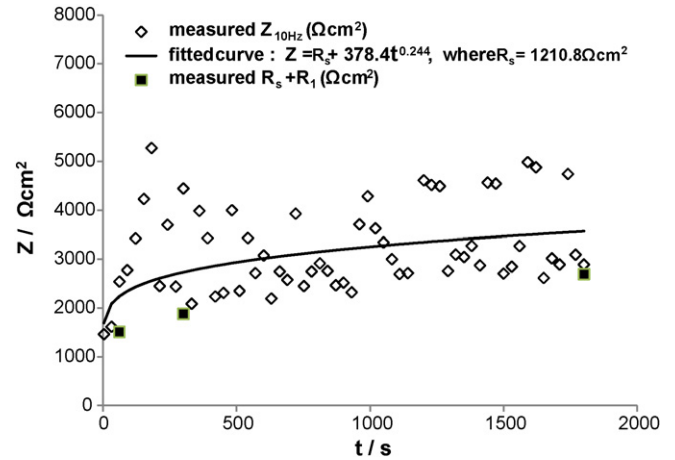


Fig. 6. Variation of the AC impedance measured at a fix frequency 10 Hz for AZ91D being dipped in an E-coating bath solution.

3.3. Electrochemical behavior in NaCl solution

The enhancement of the corrosion resistance of AZ91D in a NaCl solution by a pre-film of “electroless” E-coating can be indicated by its EIS result. The typical AC impedance spectrum of bare AZ91D in 5 wt% NaCl is presented in Fig. 7(a). There is a clear capacitive loop in the high frequency region. In the low frequency region a kind of inductive characteristic is displayed, which can be associated with the breakdown of the surface film of AZ91D in NaCl [13]. Overall, the impedance of the uncoated AZ91D is relatively small. For a pre-film covered AZ91D specimen in 5 wt% NaCl, the EIS measurements had bad reproducibility in this study. The repeatedly measured results are scattered. Nevertheless, they have some common features. Some typical impedance spectra of pre-film covered AZ91D are shown in Fig. 7(b). They appear to have only one-capacitive loop. The data points in the low frequency range are too scattered

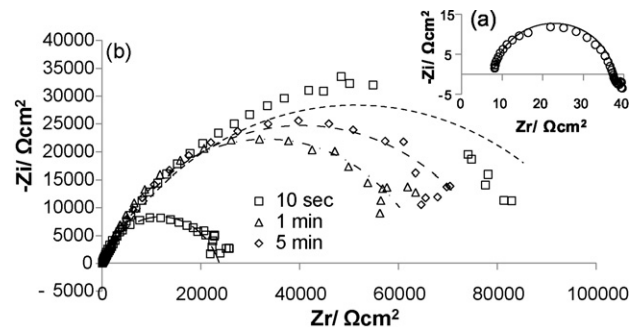


Fig. 7. AC Impedance Spectra measured in 5 wt% NaCl solution for (a) bare AZ91D and (b) AZ91D dipped in the E-coating bath for 10 s, 1 min and 5 min.

Table 2

Estimated elements of the equivalent circuit through fitting the EISs (referring to Fig. 7) of bare and pre-film coated AZ91D.

| Circuit elements | Substrate | Dipping time | | | |
|------------------------------------|-----------|--------------|--------|--------|--------|
| | | 10 s | 1 min | 5 min | 30 min |
| R_1 ($\Omega \text{ cm}^2$) | 30 | 103,000 | 66,300 | 80,700 | 23,700 |
| Q_{t1} ($\mu\text{F cm}^{-2}$) | 20 | 7.7 | 5.7 | 6.0 | 8.5 |
| Q_{p1} | 0.90 | 0.64 | 0.75 | 0.70 | 0.78 |
| R_s ($\Omega \text{ cm}^2$) | 7.7 | 27 | 130 | 150 | 39 |

to indicate anything meaningful. The diameters of these capacitive loops vary widely in repeated EIS measurements. Therefore, the dependence of the impedance of a pre-film covered specimen on dipping time cannot be successfully illustrated in this study.

Based on the EIS characteristics as shown in Fig. 7, a simple one-time-constant equivalent circuit (see Fig. 5(b)) is used to estimate the equivalent parameters. The physico-chemical explanation of this circuit will be presented later in the discussion section. Again, a constant-phase element Q is used instead of a pure capacitance in the equivalent circuit. This equivalent circuit might be too simple for simulating the EIS processes, as the bare AZ91D does show some inductive EIS characteristics and it has been theoretically and experimentally illustrated that a Mg alloy is an electrochemical system containing more than one-time-constant [12,13]. However, for a simple comparison of impedance between pre-film covered specimens, the simplification is acceptable.

Table 2 summarizes the estimated elements of the equivalent circuit, showing that the pre-film covered specimen has significantly larger resistance R and smaller capacitance Q_t than the bare AZ91D. As mentioned earlier, due to the scattered diameters of these EIS results, the dependence of the impedance on dipping time is unclear.

The observation that the impedance of the pre-film coated specimen is markedly larger than that of the bare specimen is further supported by the significantly different polarization curves of the bare and pre-film covered AZ91D in 5 wt% NaCl solution (see Fig. 8). Particularly, the cathodic polarization current densities of the pre-film covered AZ91D are more than two orders of magnitude lower than those of the bare one. The open-circuit potentials or corrosion potentials (E_{corr}) of the bare and pre-film covered AZ91D in the NaCl solution through extrapolation of their cathodic Tafel regions are listed in Fig. 8. The corrosion current density I_{corr} of the pre-film covered AZ91D is much smaller than that of the bare AZ91D. Another important finding from the polarization curves is that coat-

ing does not cause a significant change in the E_{corr} and the cathodic Tafel slope in the NaCl solution.

3.4. Corrosion damage in NaCl solution

Significant corrosion damage on bare AZ91D was observed after 3 h of immersion in the 5 wt% NaCl, while the AZ91D specimens with pre-films of “electroless” E-coating were intact under the same immersion conditions. The corrosion damage of the bare and pre-film coated AZ91D after 5 h and 24 h of immersion in the 5 wt% NaCl solution is presented in Fig. 9. Many corrosion pits can already be seen on the bare AZ91D after 5 h of immersion (Fig. 9(a)). After 24 h, severe corrosion occurred over the entire surface of the uncoated AZ91 (Fig. 9(c)). However, under the same immersion corrosion conditions, the corrosion damage of the pre-film covered AZ91D is insignificant in the first 5 h of immersion in the 5 wt% NaCl solution. No significant corrosion or coating damage is detected on its surface (Fig. 9(b)). After 24 h, only along edges is there some slight corrosion damage (Fig. 9(d)). This indicates that the pre-film of “electroless” E-coating on AZ91D offers significant corrosion protection and the pre-film covered AZ91D has much higher corrosion resistance than bare AZ91D, which is consistent with the electrochemical measurement in 5 wt% NaCl earlier.

3.5. Stability in phosphating bath

After immersion in the phosphating bath, copious amounts of gas bubbles resulting from the dissolution of bare AZ91D were generated and accumulated along the waterline region surrounding the specimen. After 4 h, in addition to the large amounts of bubbles, the phosphating solution became turbid, and the surface of AZ91D became black in color and quite rough (see Fig. 10(a)), implying that precipitation of magnesium phosphates had taken place and a phosphated layer formed there.

The pre-film of “electroless” E-coating on AZ91D significantly prevents the reaction of AZ91D with the phosphating bath solution. The solution was clear after 4 h immersion in the phosphating bath solution, and there were no significant bubbles accumulated along the waterline region. Fig. 10(b) presents its surface morphology after 4 h of immersion in the phosphating bath, which is much lighter in color than the bare AZ91D after phosphating, meaning that the pre-film covered AZ91D is much more stable than the bare AZ91D in the phosphating bath.

A quantitative characterization of the protectiveness or stability of the pre-film of “electroless” E-coating in the phosphating solution was carried out by measuring the volumes of the hydrogen evolution and the amount of dissolved magnesium ions in the phosphating bath. The results listed in Table 3 show that the amount of dissolved magnesium ions is significantly reduced by the pre-film.

No hydrogen evolution could be measured for the pre-film covered AZ91D in the first hour of immersion (Table 3). This means that there is no film damage in the first hour and the pre-film can protect the Mg alloy substrate from dissolution for a short period of time in the phosphating bath. After 4 h, hydrogen evolution can be detected from the pre-film covered specimen, but the amount of hydrogen generated from the bare specimen was about 10 times larger (Table 3). This signifies that the damage of the pre-film becomes noticeable after extended immersion in the phosphating bath solution and its protection effect decreases with immersion time.

4. Discussion

4.1. “Electroless” deposition mechanism

It is important to understand how a thin hydrophobic film can be rapidly formed on a Mg alloy surface simply by dipping the

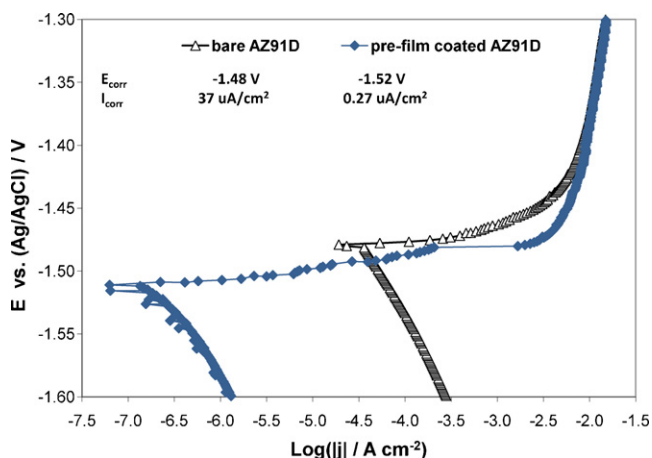


Fig. 8. Polarization curves of bare and pre-film covered AZ91D in 5 wt% NaCl solution.

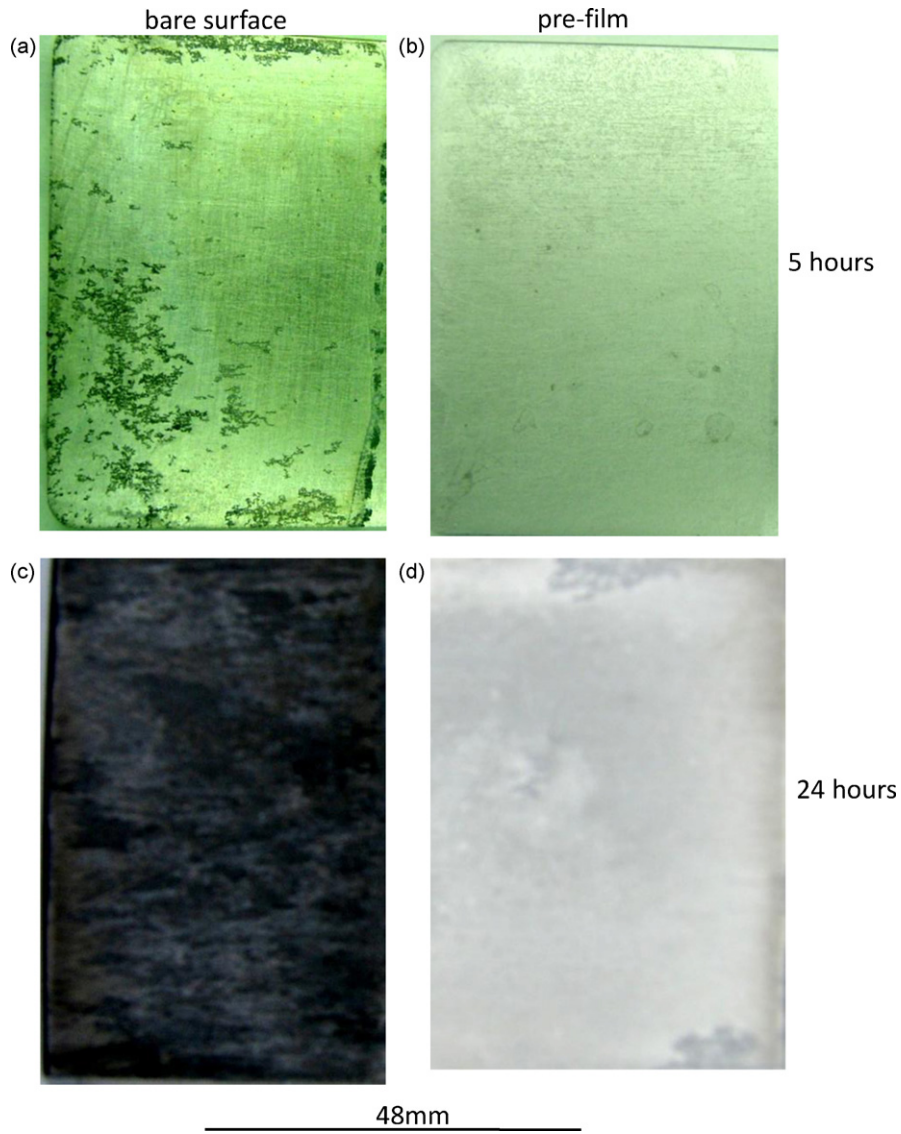


Fig. 9. surface morphologies of (a) bare AZ91D and (c) pre-film covered AZ91D after immersion in 5 wt% NaCl for (b) 5 h and (d) 24 h.

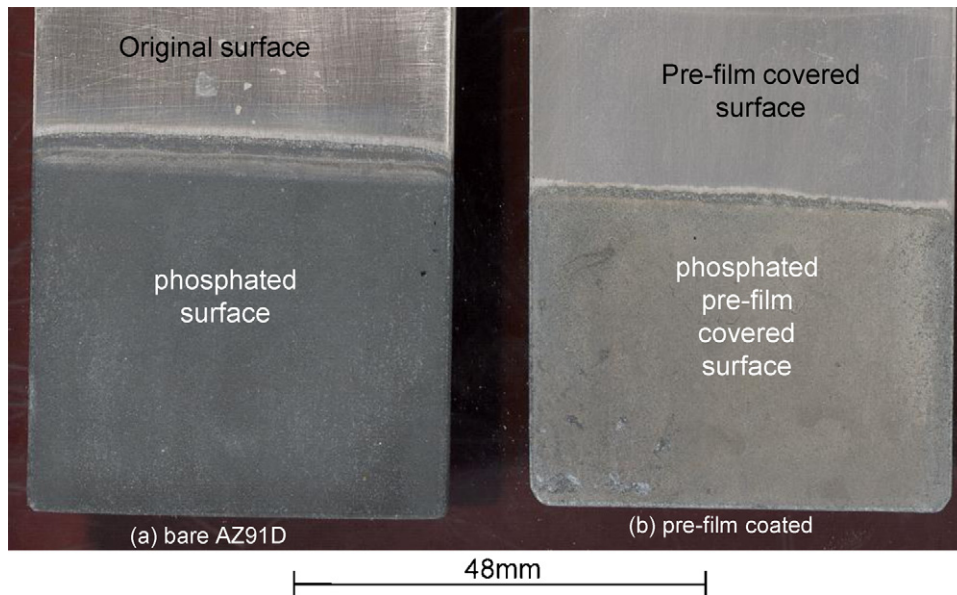


Fig. 10. Surfaces of the (a) bare and (b) pre-film covered AZ91D after immersion in a phosphating bath solution for 4 h.

Table 3

The volume of hydrogen evolution and the amount of dissolved Mg ion (Mg^{2+}) from bare and the pre-film covered AZ91D in a phosphating bath.

| Immersion time (h) | Bare surface H_2 (ml cm^{-2}) | Pre-film covered surface H_2 (ml cm^{-2}) | Bare surface Mg^{2+} (ppm) | Pre-film covered surface Mg^{2+} (ppm) |
|--------------------|---|---|-------------------------------------|---|
| 1 | 0.02 | 0.00 | | |
| 4 | 0.57 | 0.05 | 227 | 65 |

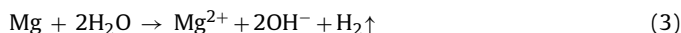
alloy in an E-coating bath solution without a current or potential applied.

It has been well known that in a normal cathodic E-coating process, apart from migration of micelles and elimination of water, the critical reactions are [14–18]:



where R-NH_3^+ is an aminoepoxy resin dissolved in the E-coating bath. Cathodic reaction (1) generates hydroxyls, resulting in an increase in pH value at the cathode surface. Reaction (2) is a pre-film of E-coating deposition or coagulation step, in which the ammonia bearing organic R-NH_3^+ reacts with the OH^- from reaction (1) and becomes an insoluble organic species R-NH_2 deposited on the cathode surface, forming an E-coat pre-film. During curing, the pre-film further polymerizes and turns into a stable insoluble hydrophobic E-coating, which is a normal E-coating widely used in industry. It should be noted that the critical species in the process is OH^- . As long as a sufficient amount of OH^- is provided, reaction (2) will continue.

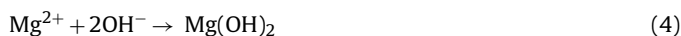
Magnesium surface always has high alkalinity in an aqueous solution because of its reaction with water [1,4]:



This is a rapid alkalization reaction. It can generate sufficient OH^- for reaction (2) on the surface of magnesium to generate a pre-film of E-coating. In this case, no reaction (1) is required, and thus no cathodic current is needed. This is the “electroless” deposition mechanism for a pre-film of E-coating on a Mg alloy [9,10], which is a result of the high surface alkalinity, a unique property of Mg [1].

According to this mechanism, this “electroless” E-coating process can only occur on Mg surfaces. Steel, galvanic steel or Al cannot generate sufficient OH^- . Thus, in this study the surfaces of steel, galvanic steel and Al coupons were found to be wet for a long time or could not be dried rapidly like an AZ91D coupon after being pulled out of the E-coating bath, and after washing their surfaces simply returned to their original states. No noticeable film was formed on their surfaces.

The involvement of reaction (3) in the “electroless” deposition of the pre-film of E-coating is also supported by the observation that a water “contaminated” AZ91D surface does not have a rapid film formation process after it is pulled out of the E-coating bath. The “contaminating” water can react with Mg (reaction (3)) first before the specimen is dipped into an E-coating bath solution. The generated OH^- and Mg^{2+} can form a $\text{Mg}(\text{OH})_2$ film on the surface:



This $\text{Mg}(\text{OH})_2$ surface film can significantly retard reaction (3) when this water “contaminated” surface is exposed to the E-coating bath solution. $\text{Mg}(\text{OH})_2$ may be dissolved to generate OH^- in the E-coating bath through the reverse process of reaction (4). However, due to the extremely low solubility of $\text{Mg}(\text{OH})_2$, about 0.9–4 mg/l in water [19], the OH^- generated in this way is not sufficient, and hence the deposition of the pre-film of E-coating (reaction (2)) cannot be initiated.

Apart from the selective “electroless” deposition and the water “contamination”, the rapid drying process for an AZ91D coupon

after removal from the E-coating bath can also be explained by the “electroless” deposition mechanism. Since the “electroless” deposited layer on AZ91D is a pre-film of E-coating, it should have a highly hydrophobic surface. The hydrophobic pre-film can expel the aqueous solution from its surface. Thus, the remaining solution on the specimen surface quickly flowed off the surface back to the solution bath, which is a process much faster than the evaporation of water from a surface. This process looks like that the surface is dried rapidly when it is gradually pulled out of an E-coat solution. Because of the hydrophobic property of the pre-film, the rinsing water could not stay on the surface either. Since no pre-film is formed on steel, galvanic steel, Al or a water “contaminated” Mg surface, their surface can keep wet for a relatively long time under the same conditions.

The above mechanism predicts that a pre-film should have a uniform coverage over the surface, because reaction (2) can suppress reaction (3), and hence the “electroless” deposition preferentially occurs in areas uncovered or covered with a thinner pre-film. The predicted uniform coverage has been experimentally observed in the study (see Figs. 1 and 2). Reaction (3) also implies that hydrogen bubbles generated during the “electroless” deposition process may be trapped in the deposited film, leaving visible pores there. This should be responsible for the tiny pores in the pre-film as shown in Fig. 2(c).

4.2. Pre-film growth kinetics

According to the “electroless” deposition mechanism, a pre-film should gradually grow with dipping time in an E-coating bath solution. The growth kinetics is schematically illustrated in Fig. 11. It is assumed that a pre-film of thickness L uniformly covers a Mg alloy AZ91D. Just like many other organic coatings, the pre-film of “electroless” E-coating on AZ91D surface is also porous. The pores can be

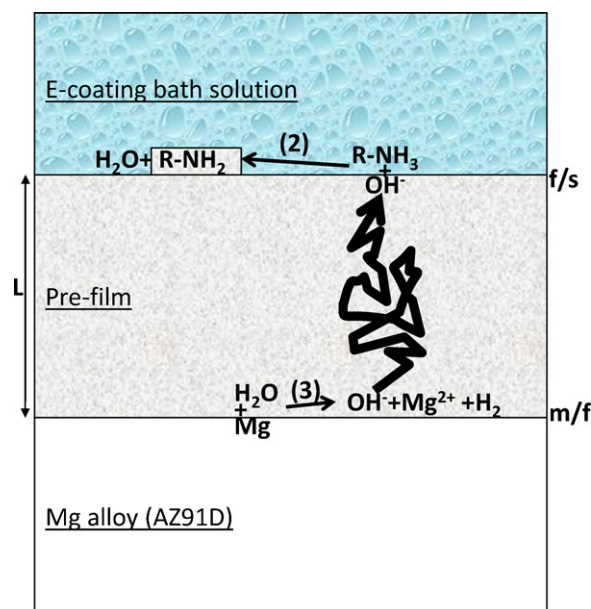


Fig. 11. Growth model for the pre-film of “electroless” E-coating on a magnesium alloy in an E-coating bath solution.

the intervals between R-NH₂ molecule trains and even those relatively large hydrogen bubble cavities mentioned earlier. They are not straight holes through the pre-film from the substrate/pre-film interface (*m/f*) directly to the pre-film/solution interface (*f/s*), but sinuous with an average sinuosity ξ in the film. It should be noted that the pore sinuosity ξ is dependent on the film thickness L . This is because that the probability for a pore to penetrate through a film directly before it bends over and twists decreases as the film becomes thicker. In a thicker film, a pore can have more bends and twists and thus a higher sinuosity. In this study, it is simply assumed that:

$$\xi = BL \quad (5)$$

where B is a constant.

During an “electroless” deposition process, alkalization reaction (3) should mainly occur at the substrate/pre-film interface *m/f*, because this reaction only occurs at a Mg alloy surface. The sufficient water contained in the pores in the pre-film next to this interface is also an essential condition for this alkalization reaction to proceed. The alkalization reaction can readily make the concentration (C_{OH}) of OH⁻ reach the saturated level of Mg(OH)₂ at the *m/f* interface. In other words, C_{OH} should be high and stable there compared with anywhere else in the pre-film.

For pre-film deposition reaction (2), the *f/s* interface should be the main site. This assumption is based on the fact that R-NH₂ is a relatively large organic molecule which is much more difficult to penetrate or transfer than a hydroxide ion in a pre-film. In addition, at the *f/s* interface, the supply of R-NH₂ is much easier than at the *m/f* interface. Therefore, the growth of the pre-film should mainly occur at the *f/s* interface and be controlled by the diffusion of OH⁻ through the film from *m/f* interface to the *f/s* interface. If the apparent diffusion coefficient of OH⁻ in the film is D , then the growth rate of the pre-film can be expressed as:

$$\frac{dl}{dt} = kDC_{OH}L \quad (6)$$

where k is a film formation constant.

It is well known that an apparent diffusion coefficient of a species in a film can be largely different from its real diffusion coefficient due to the sinuosity of its paths [20]. For a porous film containing only straight pores ($\xi = 1$), the apparent diffusion coefficient D should be proportional to the porosity θ of the film and inversely proportional to the film thickness: $D \sim \theta/L$. If the pore sinuosity ξ increases while θ keeps unchanged, then each pore path becomes longer by a factor of ξ whereas the cross-section of the path becomes smaller by the same factor, i.e., species needs to travel ξ times longer in a ξ times smaller pore. Therefore, the increase of sinuosity ξ actually slows down the diffusion rate by ξ^2 times, so the apparent diffusion coefficient can be expressed as follows

$$D = \frac{\theta D_{OH}}{\xi^2} \quad (7)$$

where D_{OH} is the real diffusion coefficient of OH⁻ in the film.

Substitution of Eq. (7) into Eq. (6) yields:

$$\frac{dl}{dt} = \frac{\kappa\theta C_{OH}D_{OH}}{L\xi^2} \quad (8)$$

Substituting Eq. (5) into it, we have:

$$\frac{dl}{dt} = \frac{\kappa\theta C_{OH}D_{OH}}{B^2L^3}$$

It is equivalent to:

$$L^3 dL = \frac{\kappa\theta C_{OH}D_{OH}}{B^2} dt$$

Its solution is:

$$L = \left(\frac{4\kappa\theta C_{OH}D_{OH}}{B^2} \right)^{1/4} t^{1/4} \quad (9)$$

which can be rewritten into:

$$\ln L = \frac{1}{4} \ln t + \frac{1}{4} \ln \left(\frac{4\kappa\theta C_{OH}D_{OH}}{B^2} \right) \quad (10)$$

Eq. (9) predicts that the pre-film grows mainly at the beginning of dipping and the growth rate decreases with dipping time. The growing kinetics of the pre-film following a power function as described by Eq. (9) or (10) is supported by the film thickness measurements (Fig. 3).

According to Eq. (10), the intercept of straight line $\ln L - \ln t$ is $4\kappa\theta C_{OH}D_{OH}/B^2$, and its slope is 1/4. As parameters k and B involved in Eqs. (9) and (10) are unknown, it is difficult to verify the reasonability of the experimentally obtained intercept. However, the power (the slope of the straight line in Fig. 3) that governs the growth kinetics of the pre-film is estimated to be 0.27 through curve-fitting of the experimental points. This value is very close to the theoretical value 1/4, suggesting that theoretically deduced kinetic Eq. (9) or (10) reasonably describes the growth of the pre-film of “electroless” E-coating.

Compared with a normal cathodic E-coat which can grow up to about 20–40 μm in few minutes, the “electroless” deposited pre-film is very thin. This is because the generation of OH⁻ by reaction (3) and its diffusion in the pre-film during “electroless” deposition are much slower than those driven by a high voltage or current in a typical E-coating process. Because of the small thickness, the pre-film is nearly transparent (Figs. 1 and 2).

4.3. In-situ impedance characterization

The growth of a pre-film with dipping time as demonstrated above is based on an ex-situ thickness measurement. It is unclear what subsequent reactions may take place in the pre-film after it is removed from the E-coating bath and exposed in air for a certain period of time. Ideally, the growth kinetics can be revealed by an in-situ technique in the E-coating bath solution directly. The Electrochemical Impedance spectroscopy (EIS) is such an in situ tool. It is believed that the evolution of the EIS spectrum of AZ91D in the E-coating bath solution with dipping time (Fig. 4) can be associated with the “electroless” deposition process of a pre-film on AZ91D.

According to the above kinetic model for a pre-film of “electroless” E-coating (Fig. 11), the pores in the pre-film should be electric current paths. Such a porous film has a typical equivalent circuit with two-time-constants as shown in (Fig. 5(a)). The elements in the equivalent circuit have the following meanings:

R_1 – The resistance of the pores in the pre-film, which can also be regarded as the overall resistance R_f of the pre-film.

Q_1 – The overall capacitance C_f of the pre-film between the substrate and the E-coating bath solution, which is determined by the composition and porosity of the pre-film and the contents in the pores.

R_2 – The reaction resistance R_t at the *m/f* interface in the pores in the pre-film, which is associated with reaction (3) on the substrate metal exposed to the water in the pores.

Q_2 – The capacitance of the *m/f* interface in the pores of the pre-film, which represents the capability of the interface for non-Faradic charging and discharging processes there. In some cases, it is simply understood as the double layer capacitance C_{dl} of the *m/f* interface in the pores.

R_3 – The solution resistance between the specimen and the reference electrode in EIS measurement.

This equivalent circuit (Fig. 5(a)) predicts that the EIS spectrum has two-capacitive loops in the Nyquist plot, which has been verified in Fig. 4. The estimated values of the equivalent elements listed in Table 1 also support that the pre-film becomes thicker with dipping time. First, the film resistance R_1 (or R_f) increases with dipping time. This can obviously be associated with an increase in film thickness. Second, the values of the film capacitance Q_1 (or C_f) after 5 min and 30 min dipping in the E-coating bath are significantly smaller than that at the first minute, also suggesting a thicker film formed after a longer dipping time. It is unclear why the capacitance at 5 min is slightly smaller than that at 30 min. Whether it is something to do with too much dissolved Mg^{2+} accumulated in the film after extended dipping still needs further investigation in the future. The relatively random dependence of R_2 and Q_2 (or R_f and C_{dl}) on the dipping might be ascribed to the non-uniformly distributed corrosion resistance over the substrate surface, which can be evidenced by the non-uniformly distributed corrosion damage pattern on the surface (Fig. 9(a)). Fortunately, Q_2 and R_2 are not directly related to the pre-film and thus not the main research interest of this study.

Since R_1 (or R_f) represents the resistance of a pre-film and its change can reflect the growth of the pre-film, it would be interesting to monitor its value during an “electroless” deposition process. The monitoring is realized through rapidly measuring the impedance $Z_{10\text{Hz}}$ at a fixed frequency 10 Hz, as $Z_{10\text{Hz}} \approx R_1$. It appears that the measured scattered $Z_{10\text{Hz}}$ points fall in a band which has a rough tendency following a power function with a power value around 1/4:

$$Z = R_s + 378.4t^{0.244} \quad (11)$$

In fact, the resistance R_f of a pre-film is film thickness L dependent:

$$R_f = \rho L/S \quad (12)$$

In this equation, ρ is film resistivity and S is surface area of a studied film. According to Eq. (9) there is:

$$R_f = \frac{\rho L}{S} = \frac{\rho}{S} \left(\frac{4\kappa\theta C_{\text{OH}} D_{\text{OH}}}{B^2} \right)^{1/4} t^{1/4} \quad (13)$$

In other words, R_f in theory is a power function of dipping time and the power value should be 1/4. This agrees with the experimental results (Fig. 6). It further supports the proposed growth kinetics of the pre-film in a “electroless” deposition process.

4.4. Corrosion resistance

From Eqs. (9) and (13), the resistivity of the pre-film can be obtained $\rho = R_f S/L = 378.4 \Omega \text{ cm}^2 / 0.948 \mu\text{m} = 3.99 \times 10^6 \Omega \text{ cm}$. Compared with a cured E-coating (far over $10^9 \Omega \text{ cm}$), this resistivity is very low. The low resistivity is understandable, because the film is an un-cured pre-film in-situ in the E-coating bath not affected by air. Its conductivity is determined by the high conductivity E-coating bath solution in the pores. In this in-situ $Z_{10\text{Hz}}$ measurement, the pre-film is deposited directly from the E-coating bath solution, so the solution in the pores of the film is a continuous liquid phase from the pores into the bulk bath. There is no interface between the solution in the pores and in the bulk bath to resist current from flowing. Fig. 12(a) schematically shows the continuity of the liquid from a pore into the bulk bath.

However, after specimen is pulled out of the E-coating bath and dried in air, at least a certain amount of water evaporates from the pore. At the same time, the pre-film surface may become passive in the air with time. When the specimen is immersed into the 5 wt% NaCl solution, due to the trapped air in the pores, the continuity between the liquid remaining in the pores and the bulk

NaCl solution will be interrupted to a great degree. This can result in a hydrophobic interface formed between the pre-film and the bulk solution. In this case, the current path is interrupted by the discontinuity of the pore liquid. The discontinuity of a pore in a pre-film caused by trapped air is schematically illustrated in Fig. 12(b). Therefore, it is expected that the film resistance R_1 (or R_f) will strikingly increase.

If the above speculation regarding the change in continuity of the pores in the pre-film is true, then the increase in R_1 will significantly enlarge the first time-constant τ_1 which may become even larger than the second time-constant of the EIS system. For example, according to the equivalent element values listed in Table 1, the first time-constant τ_1 for the EIS of AZ91D being immersed in the E-coating bath for 1 min is $\tau_1 = 612 \times 33 \times 10^{-6} \approx 0.02$ s, and the second time-constant $\tau_2 = 128 \times 709 \times 10^{-6} \approx 0.09$ s. τ_2 is more than 4 times larger than τ_1 . Hence, the capacitive loops in the high and low frequency regions respectively corresponding to τ_1 and τ_2 can be clearly separated on the Nyquist plot. However, if R_1 increases to a large value, for instance, $R_1 = 66,300 \Omega \text{ cm}^2$, a value for the pre-film in the NaCl solution (Table 2), then $\tau_1 = 66,300 \times 33 \times 10^{-6} \approx 2.2$ s, much larger than τ_2 . In this case, the capacitive loop in the low frequency region corresponding to τ_2 will be completely overwhelmed by the first capacitive loop on the Nyquist plot. A simulated evolution of EIS with an enlarged R_1 is displayed in Fig. 13. It convincingly shows that the EIS from a two-capacitive loop spectrum (Fig. 13(a)) degenerates into an apparent one-capacitive loop (Fig. 13(b)) by simply increasing the value of R_1 .

The exactly same degeneration behavior of EIS as demonstrated by the computer simulation (Fig. 13) is observed in experiments in this study for the pre-film covered AZ91D in the 5 wt% NaCl solution (Fig. 7). This means that the above speculation about the change in pore continuity in the pre-film is true, and the significantly increased resistance of the pre-film in the NaCl solution compared with that in the E-coating bath can be attributed to the formation of discontinuous pores in the pre-film and a hydrophobic pre-film surface.

Apart from the increased R_1 , the decrease in Q_1 (or C_f) is also a piece of evidence for the hydrophobic effect of the interface and the discontinuity of the liquid phase between the pre-film and the NaCl solution. It is shown in Tables 1 and 2 that the film capacitance Q_1 (or C_f) in the NaCl solution is significantly smaller than that in the E-coating solution. This leads to two inferences: (1) The hydrophobic interface between the pre-film and NaCl solution makes the pre-film have a smaller contact area with the solution. (2) The partial replacement of the liquid by air in the pores of the pre-film decreases the dielectric constant of the film (water has a much larger dielectric constant than air).

Since the EIS of the pre-film covered AZ91D in the NaCl solution actually contains two-capacitive loops, but the second one is completely overwhelmed by the first one and thus it is EIS appears to be a one-capacitive loop, there is a concern that an error may be introduced in estimating the values of R_f and Q_f by using a one-time-constant equivalent circuit (Fig. 5(b)). In Fig. 13(b), the EIS spectrum generated by a two-time-constant equivalent circuit with reasonable element values (Fig. 5(a)) is curve-fitted using a one-time-constant equivalent circuit (Fig. 5(b)). The curve-fitted pre-film resistance R and capacitance Q are very close to their actual ones. Therefore, in this study, the error caused by using a one-time-constant equivalent circuit to curve-fit the EISs of the pre-film covered AZ91D in the NaCl solution is insignificant, and the values of R and Q listed in Table 2 can truly represent the R_1 and C_f of the pre-film.

The significantly larger resistance R_1 (or R_f) of the pre-film covered AZ91D than that of the bare AZ91D (Fig. 7) in the NaCl solution implies that the pre-film of “electroless” E-coating can effectively

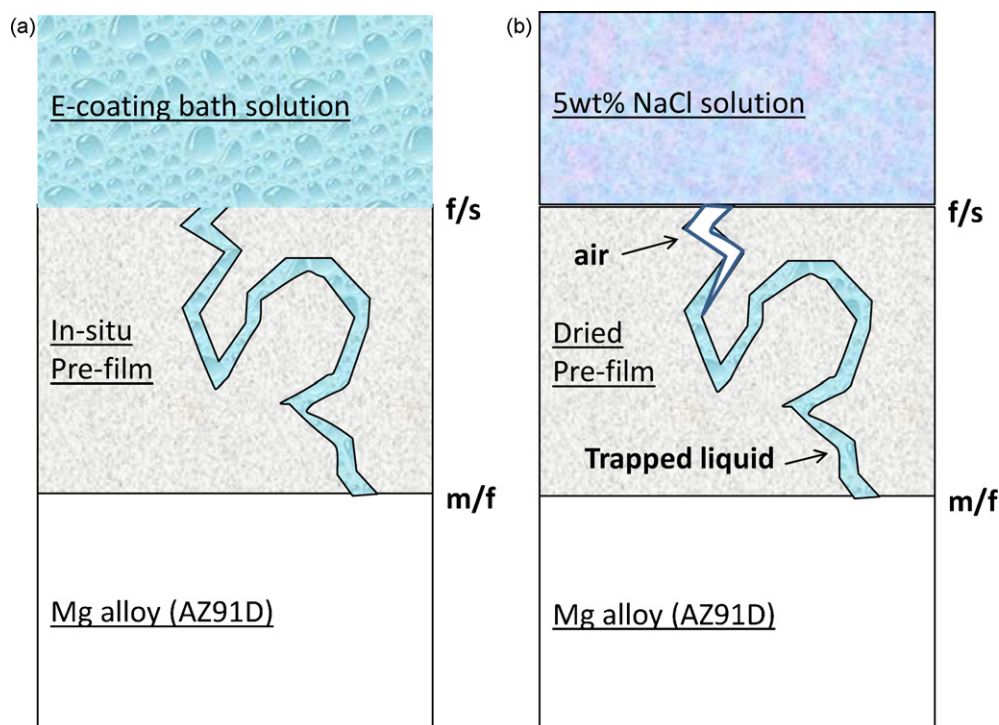


Fig. 12. Schematic illustration of a typical pore structure in a pre-film of “electroless” E-coating (a) in-situ in an E-coating bath solution and (b) after drying in air and then immersion in 5 wt% NaCl solution.

isolate the substrate from a corrosive solution and provide sufficient corrosion protection for the substrate Mg alloy. According to the above discussion, the discontinuity of the liquid in the pores in the pre-film is one of the important reasons for the corrosion protection performance of the pre-film.

In addition, the high corrosion resistance of the pre-film covered AZ91D may also be attributed to the blocking effect of the pre-film. This blocking effect is evidenced by comparison of the polarization curves of the bare and pre-film covered specimen in the NaCl solution (Fig. 8). The open-circuit potential E_{corr} is not significantly shifted by the pre-film, indicating that the film is neither anodic nor cathodic to the substrate. It is simply a barrier blocking the speci-

men surface. The significant reduction in cathodic current densities by the pre-film as shown in Fig. 8 also supports the blocking effect. Since a blocking effect cannot alter the cathodic hydrogen evolution mechanism, the bare and pre-film coated AZ91D specimens have similar cathodic Tafel slopes (see Fig. 8).

Moreover, according to the “electroless” deposition mechanism discussed earlier, R-NH₂ should be preferentially deposited at active or defect sites on the specimen surface. At a defect or active site, the higher corrosion rate of Mg than in the other areas can lead to a greater OH⁻ ion generation rate (reaction (3)), and thus lead to preferential deposition of the pre-film (R-NH₂) there, which can very effectively retard the corrosion or dissolution of the substrate. This preferential deposition of a pre-film at active or defect sites may also account for the significantly improved corrosion resistance of the pre-film covered AZ91D.

The increased corrosion resistance by a pre-film as indicated by EIS and polarization curve measurements (Figs. 7 and 8) is confirmed by an immersion test in the NaCl solution. Fig. 9 clearly demonstrates the significant improvement of corrosion resistance by the pre-film.

4.5. Stability

Although the pre-film of “electroless” E-coating can significantly inhibit the corrosion attack in the 5 wt% NaCl solution, it is unsure if this pre-film can survive in a phosphating solution. According to the “electroless” deposition mechanism, reaction (2) proceeds forward in an alkaline environment. However, in case that the environment becomes acidic, the backward reaction (2) should occur, which can result in dissolution of a deposited pre-film. Therefore, it is important learn how soon the pre-film will be dissolved and lose its protection in the phosphating solution. After the substrate Mg alloy is exposed to the phosphating solution and a significantly large area of the pre-film is dissolved, dissolution of Mg and hydrogen evolution will become evident. It is a critical concern that dissolution of a magnesium alloy part may occur in a phosphating

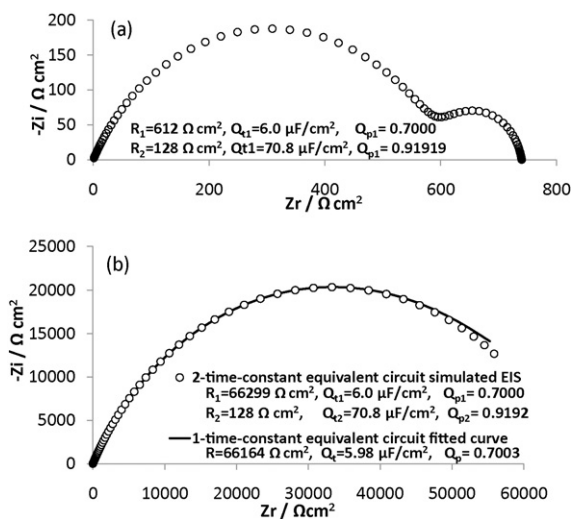


Fig. 13. (a) The simulated EIS from 0.001 Hz to 1,000,000 Hz with a two-time-constant equivalent circuit and (b) the evolution of the EIS with a dramatically increased equivalent element R_1 as well as the curve-fitting of the evolved EIS with a one-time-constant equivalent circuit.

bath during a vehicle paint process, because the dissolved Mg^{2+} ions can contaminate the phosphating bath and deteriorate the quality of phosphated layer as well as the subsequent coatings.

The results of the immersion test in the phosphating solution (Fig. 10 and Table 3) suggest that the pre-film of “electroless” E-coating offers a certain level of protection for the Mg alloy substrate in the phosphating solution. The pre-film dramatically reduces the dissolution of Mg and hydrogen evolution from AZ91D surface. After 4 h of immersion in the phosphating solution, only a small amount of Mg^{2+} and hydrogen evolution were detected from the pre-film covered AZ91D (Table 3). The damaged surface (Fig. 10(b)) after immersion indicates that the pre-film of “electroless” E-coating is only slightly damaged after 4 h of immersion in the acidic phosphating solution.

The hydrogen evolution results (Table 3) further indicate that the dissolution of AZ91D in the phosphating solution is actually too slow to cause significant damage to the pre-film in the first hour. There is no hydrogen evolution detected from the specimen surface, implying that the surface of AZ91 is still fully covered by the pre-film. In practice, a phosphating process normally only takes a few minutes. Therefore, the pre-film of “electroless” E-coating is stable enough to offer good protection for a magnesium alloy in the phosphating bath in the automotive painting line.

5. Conclusions

1. A pre-film of E-coating can be rapidly and easily self-deposited on a magnesium alloy without applying a current or voltage as a result of the surface alkalization effect of Mg in an E-coating bath solution.
2. The pre-film of E-coating can grow with dipping time and its growth kinetics is controlled by diffusion of hydroxyls in the porous pre-film.
3. The presence of the pre-film can significantly improve the corrosion resistance of the Mg alloy. It is believed that the high corrosion resistance of a pre-film in a NaCl solution is attributed to the discontinuity of pores in the pre-film.
4. The pre-film is stable enough to prevent a Mg alloy for a short period of time from dissolving in an acidic solution and to enable

a pre-film covered Mg alloy part to go through a typical phosphating process.

Acknowledgements

It is acknowledged that Mr. Sundaresan Avudaiappan and Dr. Zhenqing Xu carried out some experiments, respectively. The author would also like to thank Dr. Yar-Ming Wang, Dr. Harry Kuo, Dr. Blair Carlson and Dr. Jan Herbst for their beneficial discussion.

References

- [1] G.-L. Song, *Advanced Engineering Materials* 7 (2005) 563.
- [2] G.-L. Song, *Corrosion and Protection of Mg alloys*, Chemical Industry Press, 2006, pp.38–40, (in Chinese).
- [3] G.-L. Song, and A. Atrens, “Corrosion of Non-Ferrous Alloys. III. Mg Alloys”, An invited chapter for Volume 19B-“Corrosion and Environmental Degradation”, In Wiley-VCH series “Materials Science and Technology”, Vol.2, (2000) 131–171.
- [4] G.L. Makar, J. Kruger, *International Materials Reviews* 38 (1993) 138.
- [5] E. Aghion, B. Bronfin, Mg alloys development towards the 21st Century, *Materials Science Forum* 350–351 (2000) 19.
- [6] J. Gray, B. Luan, *Journal of Alloys and Compounds* 336 (2002) 88.
- [7] C. Blawert, W. Dietzel, E. Ghali, G. Song, *Advanced Engineering Materials* 8 (2006) 511.
- [8] W. Funke, Organic coatings in corrosion protection, in: A.D. Wilson, J.W. Nicholson, H.J. Prosser (Eds.), *Surface Coatings 2*, Elsevier Applied science, London, 1988, p. 107, Chapter 4.
- [9] G.-L. Song, *Electrochemical and Solid-State Letters* 12 (2009) D77.
- [10] G.-L. Song, Y. Wang, H. Kuo, “Self-Deposited Coatings On Magnesium Alloys” US patent application # 61/047766.
- [11] G.-L. Song, A. Atrens, D. StJohn, J. Nairn, Y. Li, *Corrosion Science* 39 (1997) 855.
- [12] G.-L. Song, A. Atrens, X. Wu, B. Zhang, *Corrosion Science* 40 (1998) 1769.
- [13] G.-L. Song, A. Bowles, D. StJohn, *Materials Science and Engineering-A* 366 (2004) 74.
- [14] F. Beck, *Progress in Organic coatings* 4 (1976) 1.
- [15] P.E. Pierce, *Journal of Coating Technology* 53 (1981) 52.
- [16] N. Vatisas, *Industrial and Engineering Chemistry Research* 37 (1998) 944.
- [17] E. Okada, H. Hosono, T. Nito, et al. “Development of High Throw power E-coat”, 2005 SAE World Congress, Detroit, (2005), SAE Technical paper #2005-01-0619.
- [18] N. Sato, “Interfacial Control Between Phosphate Films And Electrodeposition Films On Coated Steels”, SAE technical paper #900838, International Congress and Exposition, Detroit, MI (1990).
- [19] R.C. Weast, M.J. Astle, W.H. Beyer (eds), *CRC Hand book of Chemistry and Physics*, 67th edition, CRC Press, Inc, Boca Raton, Florida, (1986–1987), B-104.
- [20] Q. Cha, *Kinetics of Electrode Processes*, 2nd ed., Science Press, 1987, pp. 374 (in Chinese).